EGYPTIAN ACADEMIC JOURNAL OF

BIOLOGICAL SCIENCES ZOOLOGY

B

ISSN
2090-0759

WWW.EAJBS.EG.NET

Vol. 12 No. 1 (2020)

Citation: *Egypt. Acad. J. Biolog. Sci. (B. Zoology) Vol. 12(1) pp: 81-92(2020)*

Egypt. Acad. J. Biolog. Sci., 12(1):81-92 (2020)

Egyptian Academic Journal of Biological Sciences
B. Zoology
ISSN: 2090 – 0759
www.eajbsz.journals.ekb.eg

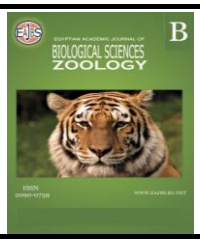

In Vivo Toxic and Teratogenic Effects of Biologically Synthesized Silver Nanoparticles in The Embryos of the Zebrafish, *Danio rerio*.

P.C. Jeba Preethi Jansi[1,*], Jeni Chandar Padua[2] and R. Regis Freeda[2]

1- Department of Zoology, Holy Cross College (Autonomous), Nagercoil, Tamilnadu, India.

2- Department of Zoology, Holy Cross College (Autonomous), Nagercoil, TN, India.

E.Mail: pc.jebapreethi@gmail.com

ARTICLE INFO

Article History
Received:15/4/2020
Accepted:6/6/2020

Keywords:
Silver Nanoparticles, Teratogenic Effects

ABSTRACT

In the current study, AgNPs synthesized using *Bacopa monnieri* were characterized by FTIR, UV-Spectrophotometry, XRD, and SEM measurements and subjected to diverse antimicrobial and toxicity assays. FTIR spectrum confirmed the involvement of amines, phenols, alkenes, amides, aromatic, and nitro compounds in the capping and reduction of AgNPs while XRD characterized the crystalline particles presenting a spherical structure around 24nm. SEM measurements showed a spherical and polygonal structure with size ranging from 35-45 nm indicating polydispersity. Comparative toxicity assays of *Bacopa monnieri* leaf extracts with nanosynthesized AgNPs on *Danio rerio* embryos, confirmed that mortality, hatchability, heartbeat rate, teratogenicity, and embryogenicity were concentration-dependent. Lethal effects were pronounced in nanosynthesised AgNPs whereas sub lethal and teratogenic toxicity effects like lordosis, scoliosis, edema and growth retardation were expressed in 84% of the exposed models. The incidence of scoliosis was found to be higher in all concentrations suggesting a possible alteration in the WNT Genes. The antimicrobial study confirmed the toxic effect of AgNPs of *B. monnieri*. This study gives newer dimensions in the furtherance of toxicity studies on green synthesized nanoparticles.

INTRODUCTION

Nanoparticles (NPs) display a wide range of applications (Krishnasamyet *et al*., 2015; Shankar *et al*; 2016; Edison *et al*., 2019; Edison *et al*., 2012) which continue to proliferate on various fronts due to their enhanced characteristics based on size, bio-distribution, and morphology (Rajeshkumar *et al*., 2015). Plant-based NPs are found to be biocompatible, swift, and, inexpensive (Huang *et al*., 2007; Edison et al., 2018; Edison *et al*., 2016). Among the huge array of metal nanoparticles, silver (Ag) nanoparticles are found to exhibit potential properties due to their high reactivity. Silver ions attach to tissue proteins causing structural alterations in the bacterial cell wall and nuclear membrane ultimately leading to cellular deformation and death (Castellano *et al*., 2007; Alsammarraie *et al*., 2018). The present study pivots around the synthesis and characterization of AgNPs using *Bacopa monnieri*, a potent medicinal plant used for cardiac, respiratory and neuropharmacological disorders (Ghosh *et al*., 2007), evaluating its antibacterial efficacy, toxicity and possible teratogenic effects using the zebrafish, *Danio rerio* preferred for its small size, transparency, rapid embryogenesis, continuous reproduction (Choi *et al*., 2016) and suitability for *in vivo* high-throughput screening (Zhao *et al*., 2009; Scown *et al*., 2010).

MATERIALS AND METHODS

Materials:

Healthy adult Zebrafishes, *Danio rerio,* were procured from the Centre for Marine Science and Technology, Manonmaniam Sundaranar University. Silver nitrate (AgNO3) was purchased from Sigma- Aldrich Laboratory, Muller Hinton agar (MHA) from Hi-media laboratories, Mumbai, India, *Staphylococcus aureus* (G+) MTCC 916 *and Klebsiella pneumoniae* (G-) MTCC 503 were collected from Microbial Type Culture Collection and Gene Bank (MTCC) Chandigarh. Milli-Q water was used throughout the experiment.

Plant Collection and Preparation of Extract:

Fresh leaves of *Bacopa monnieri* were collected, washed and shade dried for 20 days and homogenized to get a coarse powder. 5.0 gms of the powder were weighed, mixed with 100 ml of distilled water, and kept in a water bath for 1 hour at 60ºC. The filtrate was further filtered through Whatmann No.1, filter paper, and stored in refrigerated condition until further study.

Biosynthesis and Characterization of Silver Nanoparticles:

For the biosynthesis of AgNPs, a 10ml leaf extract of *B. monnieri* was added to a 90ml aqueous solution of 1mM silver nitrate for reduction into Ag+ ions and incubated overnight at room temperature. The reduction of pure Ag+ ions in aqueous solution was monitored using a UV-Vis spectrophotometer at the range of 200–800 nm. The structure of the bio-reduced AgNPs was ascertained using an X-Ray Diffraction (XRD) analyzer (Velayutham *et al*., 2012; Rajakumar *et al*., 2012). The bioactive functional groups of AgNPs were confirmed by Fourier transform infrared (FTIR) analysis (PERKIN ELMER) at the range of 4000 to 400 cm−1(Sundrarajan & Gowri, 2011; Shi *et al*., 2013). The surface morphology of the synthesized silver nanoparticles was investigated using Scanning Electron Microscopy (SEM).

Antibacterial Assay:

Klebsiella pneumoniae (Gram-negative) and *Staphylococcus aureus* (Gram-positive) was used for the antibacterial assay. Inoculums were prepared to employ aseptically adding fresh culture into 2 ml of sterile 0.145 mol/L saline tubes and the cell density was adjusted to 0.5 McFarland turbidity standard to yield a bacterial suspension of 1.5 × 108 cfu/ml. Nutrient agar medium plates were swabbed with bacterial suspension. Antibacterial activity of the biologically synthesized silver nanoparticles was tested at concentrations of 25µg, 50 µg, 75 µg, 100 µg, with Streptomycin as standard, according to Kirby Bauer well-diffusion technique. The plates were kept for incubation at 37°C for 24 hours and observed.

Zebrafish Maintenance and Embryo Selection:

Toxicity assays were accomplished using zebrafish embryos, following OECD guidelines (Guidelines, 2013). Wild-type (AB strain) male/ female 2:1 ratio were kept in aquariums in a dark room with a 12:12-hour day/night regimen. The fishes were fed with brine shrimp and blood worms. For the mating purpose, a cycle of 14 hr light/10 hr dark was imposed. Zebrafish hatching was achieved within 30 min after exposure to light in the morning. After fertilization, the embryos were carefully harvested discarding unfertilized eggs.

Toxicity Assays:

Test solutions were prepared by diluting stocks of the biosynthesized AgNPs. Thirty healthy eggs were randomly distributed into each of the 6 well plates with five different concentrations (10%, 5%, 1%, 0.5%, and 0.1%) of leaf extract and biosynthesized AgNPs by dissolving in 3 ml embryo water. The development of embryos and larvae were visualized using compound microscopes until 72 hours post-fertilization. Embryo mortality was tested at 12h, 24h, 48h, and 72hpf. The mortality rate and LC50 values were determined. Incidences

of malformations were recorded, and micrographs were taken.

Statistical Analysis:

Statistical analysis was conducted using Excel software. One-way ANOVA was used to find the significant differences between the experimental groups of embryos/larvae. The differences were considered to be statistically significant if the P-values < 0.05.

RESULTS AND DISCUSSION

Visual Inference:

The colour change pattern differed for all three solutions. Light yellow coloured leaf extract after 24 hrs incubation with 1mM AgNO3 solution resulted in dark brown colour.

UV-VIS Spectroscopy:

UV–visible spectrophotometer confirmed the formation of AgNPs in the aqueous solution. The dark brown colour of the solution indicated the reduction of silver ions. In the electron spectra, a wide peak was spotted in the area of 450 nm (Narayanan *et al*., 2010; Roucoux *et al*., 2002), confirming the formation of silver nanoparticles (Fig.1**)**. Broad Surface Plasmon Resonance (SPR) was observed in the range of 420–450 nm. The Plasmon Resonance for the sample solution was observed at 436nm which confirms the synthesis of silver nanoparticles from the biological matrix.

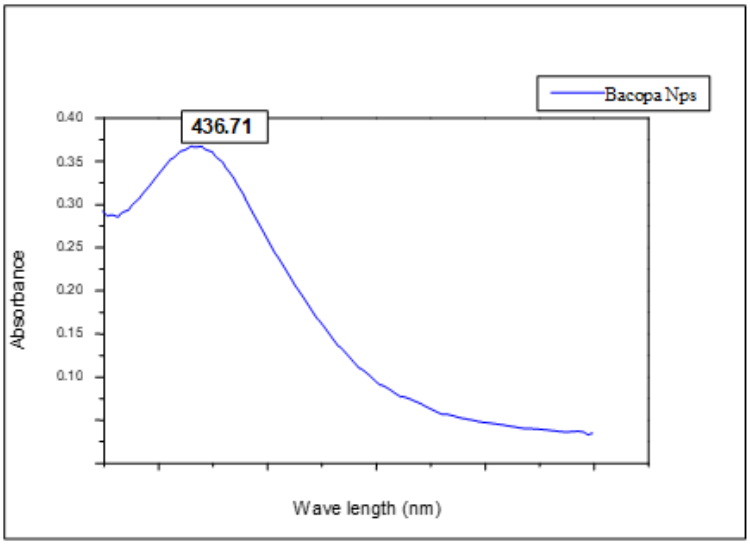

Fig 1: UV-Visible spectrum of *Bacopa monnieri* AgNPs

Fourier Transmission Infrared Spectroscopy (FT-IR):

The FTIR results showed different IR bands at 3784 cm−1, 3454 cm−1, 2362 cm−1, 1867 cm−1, 1643 cm−1, 1556 cm −1, and 1535 cm−1, 1463 cm−1, respectively for AgNPs (Fig. 2). The sharp peak at 3784 cm−1corresponds to O-H stretching of alcohol and the band at 3454 cm-1 represented –NH stretching of amide (II). The strong peak at 2362 cm-1 indicated the O=C=O stretch of the carbon dioxide. The band at 1867 cm−1 represented the occurrence of the C-H bending of an aromatic compound. Absorption at 1643 cm−1 could be due to the presence of amine groups in the synthesis process. The band at 1556 cm−1and 1535 cm−1 corresponded to strong N-O stretching of the nitro compound. The assignment at 1463 cm−1 corresponded to the C-H bending of alkane. The FTIR results confirmed the presence of –NH, –OH, O=C=O, N–O, and C–H groups, which indicated that the plant extract contained the hydroxyl and amine group-substituted flavonoids (Balashanmugam & Thangavelu, 2015). The peaks at 3454 cm−1, 1643cm−1, and 1535 cm−1 were indicating the existence of Phenols, Alkenes, and Aromatic ring stretching, respectively. The peaks range of

1650-1550 cm−1 represented the possible group of amide (Kalaiarasi *et al*., 2013). FTIR analysis had exhibited that the molecules such as phenols, amines, alkanes, and alkenes were offering stability to the AgNPs.

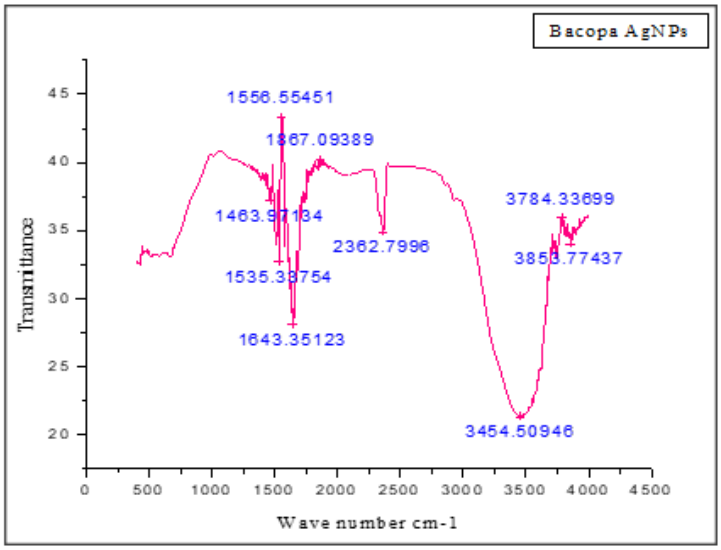

Fig 2: FTIR Spectrum of biologically synthesized AgNPs

X- Ray Diffraction (XRD):

XRD analysis of the biosynthesized AgNPs showed peaks at 2θ values of 38.1°, 44.3° and, 64.4°, respectively (Fig. 3). Moreover, the biosynthesized AgNPs were crystalline in nature. The observed patterns at 38.1°, 44.3° and 64.4° corresponded to the (111), (200) and (220) crystalline planes of the face-centered cubic structure of metallic silver (lattice constant a = 4.086 A◦, was matched well with Joint Committee on Powder Diffraction Standards (JCPDS) values). The average particle size was determined by Scherrer's formula (Cullity & Stock, 2014).

$$d=0.9\ \lambda/\ \beta\ \text{Cos}\ \theta$$

Where, d represent NPs' mean diameter, λ show X-ray radiation wavelength, β signify XRD peak at the diffraction angle θ. The observed peaks were well in agreement with the JCPDS card no. 03-0921which implies that the particles are crystalline with a spherical structure and the estimated particle size around 24 nm (Fig.4) which was found to be consistent with the results of studies by other researchers (Chen & Kimura, 2001; Anandalakshmi *et al*., 2015).

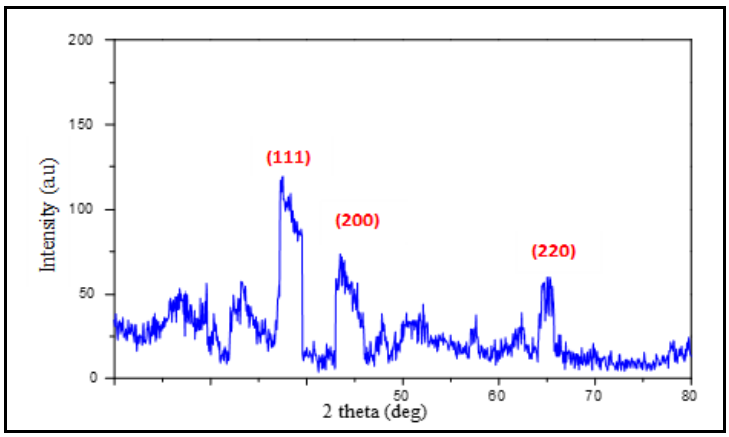

Fig 3 : XRD patterns of AgNPs synthesized using *B. monnieri* extract

Scanning electron microscope analysis of silver nanoparticles

Scanning Electron Microscopy (SEM) analysis revealed the shape of the biosynthesized AgNPs as spherical and polygonal (Fig. 4). The mean size of the AgNPs was found to be in the range of 35-45 nm indicating polydispersity. Formations of aggregated particles were observed which could be due to the existence of phytochemicals in the extract (Santhoshkumar *et al*., 2019).

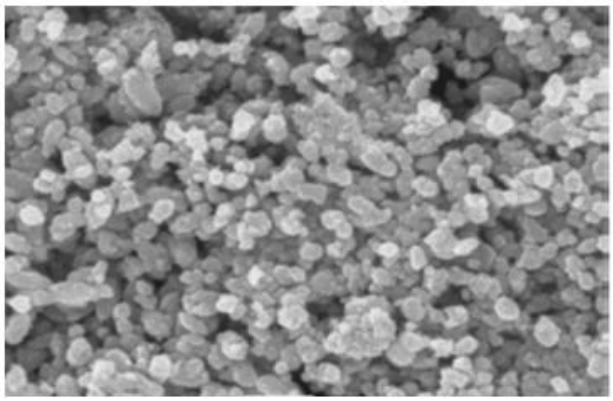

Fig 4: SEM image of AgNPs obtained by reduction of $AgNO_3$ with *B. monnieri*

Antibacterial Assay:

Using the Kirby Bauer well diffusion method antibacterial efficacy of different concentrations of the biosynthesized AgNPs Viz. 25µl, 50 µl, 75µl, and 100 µl was well observed in terms of a clear zone of inhibition (Fig. 5). The Bio AgNPs showed inhibition zones in all the concentrations against the two bacterial strains. In all bacterial strains, the zone of inhibition increased with an increase in concentrations of biosynthesized silver nanoparticles.

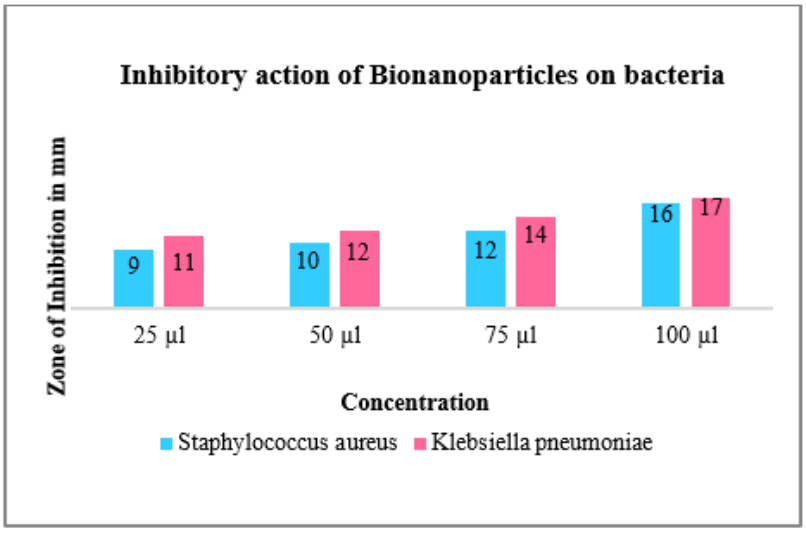

Fig 5: Graph showing the antibacterial activity of *B. monnieri* coated AgNPs on bacteria

The silver nanoparticle synthesized using leaf extract at 100 µg/ml showed the maximum antimicrobial effect on *Klebsiella* (17 mm) and *Staphylococcus* (16 mm). The highest level of inhibition (17 mm) was observed in *Klebsiella* at the concentration of 100 µl and the lowest level of inhibition (9 mm) was found in *S. aureus* at the concentration of 25

µl. In the case of *Klebsiella*, AgNPs at the concentration of 100µl showed greater potential and effectivity as compared to the standard drug Streptomycin. Comparatively, in the case of *S. aureus*, 100 µl concentration was found to be more efficient than Streptomycin. Compared to *Klebsiella pneumoniae*, *S. aureus* was less affected by biologically synthesized AgNPs even in high concentrations.

Toxicity Assays on the embryos of *Danio rerio*:

LC50 values (Fig.6) were assessed. The mortality, hatchability, heartbeat (Fig.7), teratogenicity, and malformations (Fig.8) at different stages were observed and compared with control embryos (Tables 1a and 1b). The mortality of Zebrafish embryos on exposure to *B. monnieri* leaf extract and biosynthesized AgNPs exposure is shown in Fig.7A. Mortality was recorded at 12, 24, 48, and 72 hpf in the order of increasing concentration. Compared with the control group, no significant difference existed in the leaf extract concentration group of 1% and below, but a notable difference was observed at concentrations of 5% and 10%. A high number of mortalities were observed in AgNPs in all concentrations. The median lethal concentration (LC50) of bio AgNPs was calculated based on the zebrafish mortality curves (Fig. 6). The LC50 was observed at 0.5% (0.47). The significant indicator of hatchability is the dechorionization of the embryo. Zebrafish embryos begin to hatch at 48 hpf and finish hatching at 72 hpf in normal condition (Huang *et al*., 2018). Hatching rate between control and low concentration (0.1% and 0.5%) had no obvious difference. The rate is reduced in the higher groups (1%, 5%, and 10%) for leaf extract. However, the embryo-hatching rate was significantly reduced in the AgNPs exposure groups, with hatching rates of 53% in the 0.5% and no hatching was observed in further concentrations (Fig.7B). These data indicated a remarkable dose-dependent decrease in the hatching rate in the leaf extract and biosynthesized AgNPs treated groups compared with those of the control. As shown in figure 7C, heart rate changes were found in a dose-dependent manner with leaf extract and biosynthesized AgNPs exposure, compared with the control group. While comparing the results, the heartbeat rate is decreased, when the extract concentration increases. The normal heartbeat of larvae is around 155 times/min (Huang *et al*., 2018). All the exposure groups exhibited slower heart pumps, and AgNPs of 0.5% showed significantly abnormal heart rates of approximately 106 times/min.

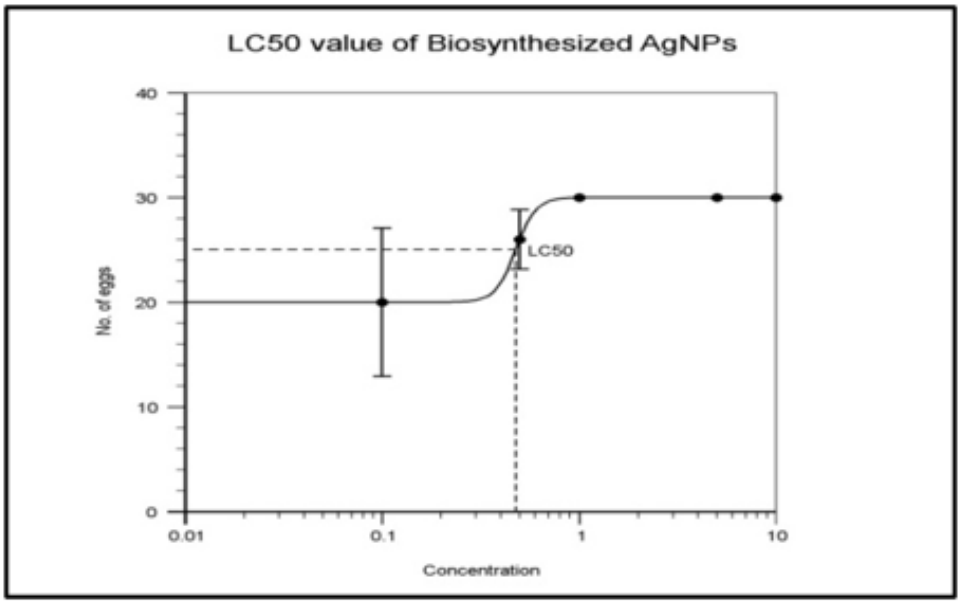

Fig 6: LC50 value of biosynthesized AgNPs on Zebrafish embryos

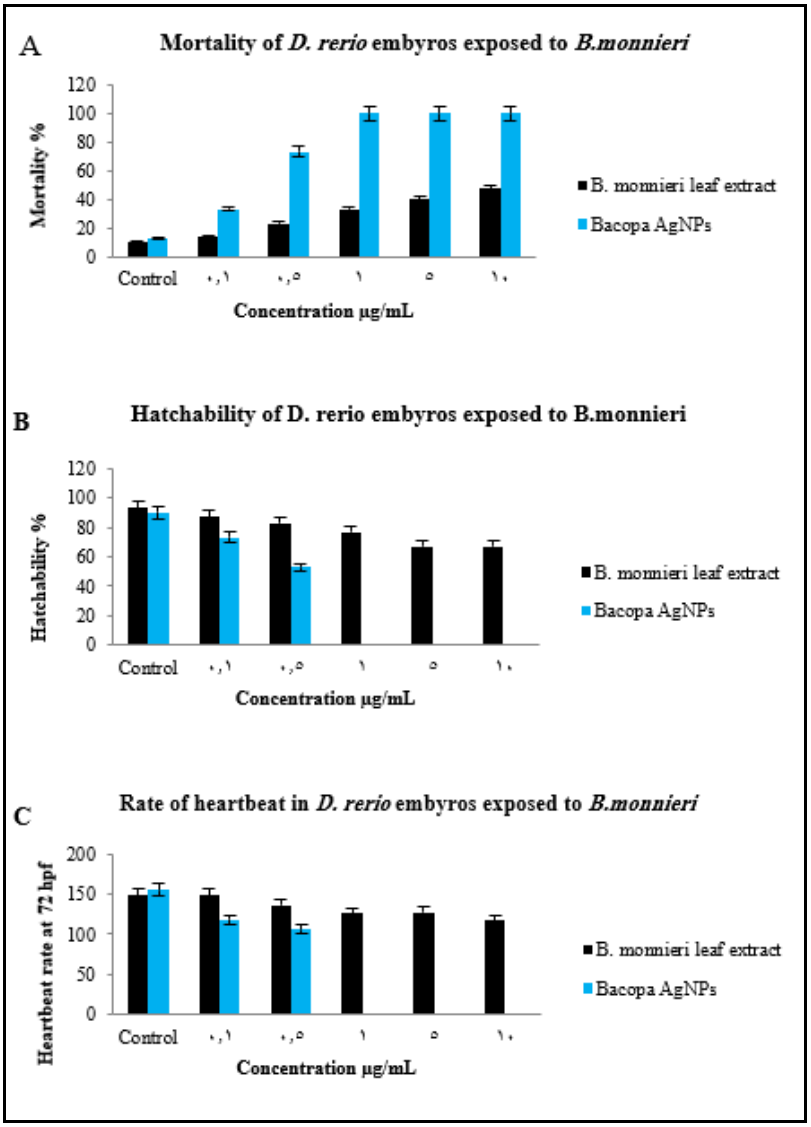

Fig 7: Graph representing the toxicity of *B. monnieri* and biosynthesized AgNPs in terms of (A) mortality, (B) hatchability, and (C) heart rate in zebrafish embryos. Data are represented as mean ± standard of three independent experiments.

Teratogenicity of Zebrafish Embryos:

A series of morphological deformations were observed under the stimulation of leaf extract and biosynthesized AgNPs including pericardial edema, yolk sac edema, lordosis, tail malformation, tail curvature, head malformation, and scoliosis. Teratogenicity increased in a concentration-dependent manner. The most prominent malformations were tail malformation and pericardium edema. The tails showed a sharp kink in the middle of the tail length combined with a turn in the tail orientation (Fig.8M) (Klempt, 2012). The control embryos appeared normal throughout the observation period. The result obtained from mortality studies confirms the effects of the leaf extract and nanosynthesized leaf extract. The mortality rate was increased incredibly to a large extent in biosynthesized AgNPs which might be due to the accumulation of silver nanoparticle which could have been toxic to the developing embryos.

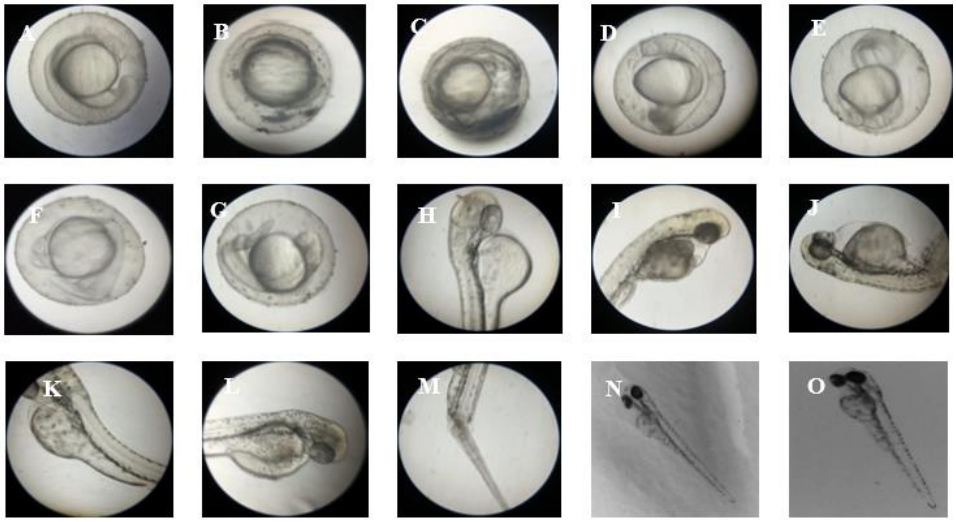

Fig 8. Microscopic images of normal control embryo at (A) 24 hpf (B) Coagulated egg (C) Coagulated embryo at 36h (D) Embryo with deformed tail (E-G) Embryos with tail malformations (H) embryo showing yolk sac edema at 48h (I) head malformed embryo at 60h (J) Pericardial edema and bent tail at 60h (K) Scoliosis (L) Abdominal edema at 72h (M) Embryo having twisted tail at 72 hpf (N-O) normal embryo at 48hpf and 72hpf.

Table 1a: Teratogenicity chart of *D.rerio* embryos

Type of toxicity	Control	*B. monnieri* leaf extract	Biosynthesized AgNPs
Lethal			
Coagulation	-	+	+++
Lack of heartbeat	-	+	++
Sublethal			
Pericardial edema	-	+	+
Yolk sac edema	-	+	++
Tail deformation	-	+	++
Reduced heart rate	-	++	++
Teratogenic			
Tail malformation	-	+	+++
Head malformation	-	-	+
Scoliosis	-	-	+
Tail length	-	+	+

Table 1b: showing toxicological endpoints at different stages of development of zebrafish embryos (hpf)

Types of toxicity	Exposure time							
	B. monnieri leaf extract				Biosynthesized AgNPs			
	12h	24h	48h	72h	12h	24h	48h	72h
Lethal endpoints								
Coagulation	*	*			*	*	*	
No heartbeat			*	*			*	*
Sublethal developmental endpoints								
Formation of somites	*				*	*		
Spontaneous movements		*				*	*	
Heartbeat frequency				*			*	*
Edema			*			*	*	*
Endpoints of Teratogenicity								
Malformation of the head			*				*	*
Malformation of the tail			*	*		*	*	*
Tail length				*			*	*
Scoliosis				*			*	*

Statistical Analysis:

Teratogenic data were presented as the mean ± SD (triplicate assays). Statistical analysis was done using Excel. ANOVA tests corroborate a calculated p-value of 0.03, p-value of less than 0.05 ($p < 0.05$). Hence, it was accepted as statistically significant between experimental and control groups.

CONCLUSION

In conclusion, *B. monnieri* leaf extract and biosynthesized AgNPs caused a dose-dependent increase in developmental damage in zebrafish embryos. Mortality, hatchability, heartbeat rate, and teratogenic effects proved that biosynthesized extract showed more lethality when compared with the leaf extract of *B. monnieri*. The toxicity of biosynthesized AgNPs in zebrafish embryos could also be due to the deposition of nanoparticles inside the cell nucleus which led to the observed toxicity through several mechanisms such as DNA damage and chromosomal aberrations. Our results primarily revealed that the incidence of tail malformation is more in zebrafish embryos with increasing concentration. This could be due to Wnt genes that play a significant role in body patterning, cell proliferation/differentiation, and tumorigenesis by acting at the cell surface or on the extracellular matrix to mediate cell-cell signaling (Shimizu *et al*., 2005; Kelly *et al*., 1995). The genes, Wnt3a and Wnt8a play a vital function in body patterning during early embryogenesis. Inhibition of Wnt8a in zebrafish results in posterior body reduction and expansion of dorsal axial tissues, indicating that it is involved in the formation of the paraxial mesoderm and tail (Shimizu *et al*., 2005; Erter *et al*., 2001; Lekven *et al*., 2001). Loss of Wnt8a function has also been reported to prevent tail development (Agathon *et al*., 2003).Wnt3a and Wnt8a regulate the number of downstream genes, like ventrally expressed homeobox genes and cdx genes to mediate the Wnt signals. As Wnt signaling plays a crucial role in body patterning during early vertebrate embryogenesis, the up- or down-regulation of Wnt genes could induce unusual body patterning of the zebrafish embryo, thus scoliosis, head malformation, curved tail, twisted tail, and tail malformation were observed after exposure to *B. monnieri* leaf extract and biosynthesized AgNPs during this study. Hence, even though *B. monnieri* is safe to be consumed due to its potential pharmaceutics, it exhibits mild toxic activity on a higher concentration as evaluated in the zebrafish embryo model. There is a need for further research to know and explain the mechanisms that induce specific teratogenicity in Zebrafish embryos.

Conflicts of Interest:

The authors declare that they have no conflicts of interest with the contents of this article.

Acknowledgement

This research did not receive any specific grant from funding agencies in the public, commercial, or not-for-profit sectors.

REFERENCES

Agathon, A., Thisse, C. and Thisse, B. (2003). The molecular nature of the zebrafish tail organizer. *Nature* 424, 448–452. https://doi.org/10.1038/nature01822.

Alsammarraie, F.K., Wang, W., Zhou, P., Mustapha, A. and Lin, M. (2018). Green synthesis of silver nanoparticles using turmeric extracts and investigation of their antibacterial activities. *Colloids and Surfaces B: Biointerfaces*, 171, 398–405. https://doi.org/ 10. 1016/j.colsurfb.2018.07.059.

Anandalakshmi, K., Venugobal, J. and Ramasamy, V. (2015). Characterization of silver nanoparticles by green synthesis method using *Pedalium murex* leaf extract and their antibacterial activity. *Applied Nanoscience*, 6(3), 399–408, https://doi.org/ 10. 1007/

s13204-015-0449-z.

Balashanmugam, P. & Thangavelu, K. (2015). Biosynthesis characterization of silver nanoparticles using *Cassia roxburghii* DC. aqueous extract, and coated on cotton cloth for effective antibacterial activity. *International Journal of Nanomedicine*, 87. https://doi.org/10.2147/ijn.s79984.

Castellano, J.J., Shafii, S.M., Ko, F., Donate, G., Wright, T.E., Mannari, R.J. and Robson, M.C. (2007). Comparative evaluation of silver-containing antimicrobial dressings and drugs. *International Wound Journal*, 4(2), 114–122.

Chen, S. & Kimura, K. (2001). Synthesis of thiolate-stabilized platinum nanoparticles in Protolytic solvents as isolable colloids. *Journal of Physical Chemistry* B 105 5397–5403. https://doi.org/ 10.1021/jp0037798.

Choi, J.S., Kim, R.O., Yoon, S. and Kim, W.K. (2016). Developmental toxicity of zinc oxide nanoparticles to Zebrafish (*Danio rerio*): a transcriptomic analysis. *PLoS One*. 11 (8). https://doi.org/10.1371/journal.pone.0160763.

Cullity, B.D. & Stock, S.R. (2014). Elements of X-ray Diffraction, Pearson Education, 656 pages.

Edison, T.J.I. & Sethuraman, M. (2012). Instant green synthesis of silver nanoparticles using *Terminalia chebula* fruit extract and evaluation of their catalytic activity on reduction of methylene blue. *Process. Biochemistry* 47 (9) 1351–1357.

Edison, T.N.J.I., Atchudan, R., Sethuraman, M.G. and Lee, Y.R. (2016). Super capacitor performance of carbon supported Co3O4 nanoparticles synthesized using *Terminalia chebula* fruit. *Journal of the Taiwan Institute Chemical Engineers* 68 489–495. https://doi.org/ 10.1016/ j.jtice.2016.09.021.

Edison, T.N.J.I., Atchudan, R. and Lee, Y.R. (2018). Binder-free electro-synthesis of highly ordered nickel oxide nanoparticles and its electrochemical performance. *Electrochim. Acta* 283 1609–1617. https://doi.org/10.1016/j.electacta.2018.07.101.

Edison, T.N.J.I., Atchudan, R. and Lee, Y.R. (2019). Facile synthesis of carbon encapsulated RuO nanorods for supercapacitor and electrocatalytic hydrogen evolution reaction. *International Journal of Hydrogen Energy* 44 (4) 2323–2329. https://doi.org/ 10.1016/ j.ijhydene. 2018.02.018.

Erter, C.E., Wilm, T.P., Basler, N., Wright, C.V.E. and Solnica-Krezel, L. (2001). Wnt8 is required in lateral mesendodermal precursors for neural posteriorization in vivo. *Development* 128, 3571–3583.

Ghosh, T., Maity, T., Das, M., Bose, A. and Dash, D. (2007). In Vitro antioxidant and hepatoprotective activity of ethanolic extract of *Bacopa monnieri* Linn. Aerial parts. *Iranian Journal of Pharmacology and Therapeutics.* 6. 77-85.

Guidelines, O. (2013). The F.O.R., Of, T., Test No. 236: fish embryo acute toxicity (FET) test 1–22. https://doi.org/10.1787/9789264203709-en.

Huang, J., Li, Q., Sun, D., Lu, Y., Su, Y., Yang, X., Wang, H., Wang, Y., Shao, W., He, N., Hong, J. and Chen, C. (2007). Biosynthesis of silver and gold nanoparticles by novel sundried *Cinnamomum camphora* leaf. *Nanotechnology.* 18. https://doi.org/105104. 10.1088/0957-4484/18/10/105104.

Huang, D., Li, H., He, Q., Yuan, W., Chen, Z. and Yang, H. (2018). Developmental Toxicity of Diethylnitrosamine in Zebrafish Embryos/Juveniles Related to Excessive Oxidative Stress. *Water, Air, & Soil Pollution*, 229(3).

Kalaiarasi, R., Prasannaraj, G. and Venkatachalam, P. (2013). A rapid biological synthesis of silver nanoparticles using leaf broth of *Rauvolfia tetraphylla* and their promising antibacterial activity, *Indo American Journal of Pharmaceutical Research* 3 (10) 8052–8062. https://doi.org/1 0.1044/1980-iajpr.00998..

Kelly, G.M., Greenstein, P., Erezyilmaz, D.F. and Moon, R.T. (1995). Zebrafish wnt8 and

wnt8b share a common activity but are involved in distinct developmental pathways. *Development* 121, 1787–1799.

Klempt, M. (2012). 353-nonylphenol induces expression of the t-box6 gene in zebrafish embryos linking transcriptional information with deformities. *Journal of Fisheries Sciences. com*. https://doi.org/10.3153/jfscom.2013004.

Krishnasamyet, A., Sundaresan, M. and Velan, P. (2015). Rapid phytosynthesis of nano-sized titanium using leaf extract of *Azadirachta indica*. *International Journal of ChemTech Research* 8 (4) 2047–
2052.

Lekven, A.C., Thorpe, C.J., Waxman, J.S. and Moon, R.T. (2001). Zebrafish wnt8 Encodes Two Wnt8 Proteins on a Bicistronic Transcript and Is Required for Mesoderm and Neurectoderm Patterning. *Developmental Cell* 1, 103–114. https://doi.org/10.1016/S1534-5807(01)00007-7.

Narayanan, K.B. & Sakthivel, N. (2010). Phytosynthesis of gold nanoparticles using leaf extract of *Coleus amboinicus* Lour. *Materials Characterization*, 61(11), 1232–1238. https://doi.org/10.1016/j.matchar.2010.08.003.

Rajakumar, G., Rahuman, A.A., Priyamvada, B., Khanna, V. G., Kumar, D. K. and Sujin, P.J. (2012). *Eclipta prostrata* leaf aqueous extract mediated synthesis of titanium dioxide nanoparticles. *Materials Letters*, 68, 115–117. https://doi.org/10.1016/j.matlet.2011.10.038

Rajeshkumar, S., Nagalingam, M., Ponnanikajamideen, M., Vanaja, M. and Malarkodi, C.S. (2015). Anticancer activity of *Andrographis paniculata* leaves extract against Neuroblastima (Imr-32) and Human colon (Ht-29) Cancer cell line. *World Journal of Pharmacy And Pharmaceutical Sciences*. 4.

Roucoux, A., Schulz, J. and Patin H. (2002). Reduced transition metal colloids: a novel family of reusable catalysts?. *Chemical Reviews* 102 3757–3778. https://doi.org/10.1021/cr010350j.

Santhoshkumar, J., Sowmya, B., Venkat Kumar, S. and Rajeshkumar, S. (2019). Toxicology evaluation and Antidermatophytic activity of silver nanoparticles synthesized using leaf extract of *Passiflora caerulea*. *South African Journal of Chemical Engineering*. https://doi.org/10.1016/j.sajce.2019.04.001.

Scown, T., Van Aerle, R. and Tyler, C. (2010). Do engineered nanoparticles pose a significant Threat to the aquatic environment? *Critical Reviews of Toxicology*, 40 (7) 653–670. https://doi.org/10.3109/10408444.2010.494174.

Shankar, P.D., Shobana, S., Karuppusamy, I., Pugazhendhi, A., Ramkumar, V.S., Arvindnarayan, S. and Kumar, G. (2016). A review on the biosynthesis of metallic nanoparticles (gold and silver) using bio-components of microalgae: Formation mechanism and applications. *Enzyme and Microbial Technology*, 95. 28-44. https://doi.org/10.1016/j.enzmictec.2016.10.015.

Shi, H., Magaye, R., Castranova, V. and Zhao, J. (2013). Titanium dioxide nanoparticles: *a review of current toxicological data, Part. Fibre Toxicol.* 10 (1) 15.

Shimizu, T., Bae, Y.K., Muraoka, O. and Hibi, M. (2005). Interaction of Wnt and caudal related genes in zebrafish posterior body formation. *Developmental Biology*, 279, 125–14. https: //doi.org/10.1016/j.ydbio.2004.12.007.

Sundrarajan M & Gowri S. (2011). Green Synthesis of Titanium Dioxide Nanoparticles by *Nyctanthes Arbor-Tristis* Leaves Extract. Chalcogenide Lett., 8 (8), 447–451.

Velayutham, K., Rahuman, A.A., Rajakumar, G., Santhoshkumar, T., Marimuthu, S., Jayaseelan, C., Bagavan, A., Kirthi, A.V., Kamaraj, C. and Zahir, A.A. (2012). Evaluation of *Catharanthus roseus* leaf extract-mediated biosynthesis of titanium Dioxide nanoparticles against *Hippobosca maculata* and *Bovicola ovis*. *Parasitology*

Research,111 (6) 2329–2337. https://doi.org/10.1007/s00436-011-2676-x.

Zhao, J., Bowman, L., Zhang, X., Vallyathan, V., Young, S.H., Castranova, V. and Ding, M. (2009). Titanium dioxide (TiO2) nanoparticles induce JB6 cell apoptosis through activation of the caspase-8/Bid and mitochondrial pathways. *Journal of Toxicology and Environment Health Part A* 72 (19) 1141–1149. https://doi.org/10.1080/15287390903091764.